(2)

NAVAL POSTGRADUATE SCHOOL
Monterey, California

THESIS

CROSS-SHORE SEDIMENT TRANSPORT ON A NATURALLY BARRED BEACH

by

Randall T. Humiston

March 1993

Thesis Advisor: Edward B. Thornton
Second Reader: Thomas C. Lippmann

Approved for public release; distribution is unlimited.

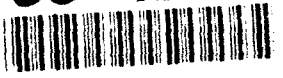

REPORT DOCUMENTATION PAGE

Form Approved
OMB No 0704-0188

1. AGENCY USE ONLY (Leave blank)	2. REPORT DATE	3. REPORT TYPE AND DATES COVERED
	March 1993	Master's Thesis

4. TITLE AND SUBTITLE
CROSS-SHORE SEDIMENT TRANSPORT ON A NATURALLY BARRED BEACH

5. FUNDING NUMBERS

6. AUTHOR(S)
Humiston, Randall T.

7. PERFORMING ORGANIZATION NAME(S) AND ADDRESS(ES)
Naval Postgraduate School
Monterey, CA 93943-5000

8. PERFORMING ORGANIZATION REPORT NUMBER

9. SPONSORING / MONITORING AGENCY NAME(S) AND ADDRESS(ES)

10. SPONSORING / MONITORING AGENCY REPORT NUMBER

11. SUPPLEMENTARY NOTES
The views expressed in this thesis are those of the author and do not reflect the official policy or position of the Department of Defense or the U.S. Government.

12a. DISTRIBUTION / AVAILABILITY STATEMENT
Approved for public release, distribution is unlimited

12b. DISTRIBUTION CODE

13. ABSTRACT *(Maximum 200 words)*

Bailard's sediment transport model (1981) is evaluated using field data obtained on a naturally barred beach. Principal field measurements consist of a cross-shore array of bi-directional current meters spanning the surf zone and daily bathymetric surveys. The model predicts bed and suspended load transport separately based on various velocity moments. The velocities are partitioned into mean currents, long waves (< 0.05 Hz) and short waves (> 0.05 Hz) to determine their relative importance to the transport. Velocity moments are then computed over 90 minute intervals to resolve tidal fluctuations. Finally, predicted transport rates are integrated and compared with daily cross-shore bathymetric profiles (averaged over a 400m length of beach).

Results indicate that suspended load was consistently greater than bed load, as much as an order of magnitude during episodes of large incident waves, owing to the slow fall velocity (2cm/s) of the fine grain sand within the surf zone. The contribution by the mean current, long and short waves to the cross-shore transport were of the same order. Variance of transport during all stages of tide and over a range of incident waves were consistently greater in the vicinity of the bar and trough than

14. SUBJECT TERMS	15. NUMBER OF PAGES
Sediment transport, DELILAH, Cross-shore transport	47
	16. PRICE CODE

17. SECURITY CLASSIFICATION OF REPORT	18. SECURITY CLASSIFICATION OF THIS PAGE	19. SECURITY CLASSIFICATION OF ABSTRACT	20. LIMITATION OF ABSTRACT
Unclassified	Unclassified	Unclassified	UL

#13 ABSTRACT (CONTINUED)

seaward of the bar and on the beach face. Tidal signatures were apparent in all modes of transport. The model appeared to under-predict measured bathymetry during low-energy periods and over-predict during high-energy conditions. However, the model does correctly predict the first order movement of the bar.

Approved for public release; distribution is unlimited.

CROSS-SHORE SEDIMENT TRANSPORT ON A NATURALLY BARRED BEACH

by

Randall T. Humiston
Lieutenant, United States Navy
B.S., University of Illinois at Carbondale, 1984

Submitted in partial fulfillment
of the requirements for the degree of

MASTER OF SCIENCE IN PHYSICAL OCEANOGRAPHY
AND METEOROLOGY

from the

NAVAL POSTGRADUATE SCHOOL
March 1993

Author: _____
Randall T. Humiston

Approved by: _____
Edward B. Thornton, Thesis Advisor

_____
Thomas C. Lippmann, Second Reader

_____
Curtis A. Collins, Chairman
Department of Oceanography

ABSTRACT

Bailard's sediment transport model (1981) is evaluated using field data obtained on a naturally barred beach. Principal field measurements consist of a cross-shore array of bi-directional current meters spanning the surf zone and daily bathymetric surveys. The model predicts bed and suspended load transport separately based on various velocity moments. The velocities are partitioned into mean currents, long waves (< 0.05 Hz) and short waves (> 0.05 Hz) to determine their relative importance to the transport. Velocity moments are then computed over 90 minute intervals to resolve tidal fluctuations. Finally, predicted transport rates are integrated and compared with daily cross-shore bathymetric profiles (averaged over a 400m length of beach).

Results indicate that suspended load was consistently greater than bed load, as much as an order of magnitude during episodes of large incident waves, owing to the slow fall velocity (2cm/s) of the fine grain sand within the surf zone. The contribution by the mean current, long and short waves to the cross-shore transport were of the same order. Variance of transport during all stages of tide and over a range of incident waves were consistently greater in the vicinity of the bar and trough than seaward of the bar and on the beach face. Tidal signatures were apparent in all modes of

transport. The model appeared to under-predict measured bathymetry during low-energy periods and over-predict during high-energy conditions. However, the model does correctly predict the first order movement of the bar.

TABLE OF CONTENTS

LIST OF TABLES

LIST OF FIGURES

ACKNOWLEDGEMENTS

I would like to express my special appreciation and thanks to Mary Bristow, Naval Postgraduate School, whose tireless efforts and inhuman tolerance of my computer illiteracy facilitated timely and accurate completion of data processing.

To my wife, Cheryl, words alone cannot express how much I appreciate your undying support and faith in me. Your continual encouragement, especially during the many nights alone and my short temper, can never be adequately repaid. Thank you, I love you.

This work was funded by ONR Coastal Studies Grant N00014-92-AF-0002.

I. INTRODUCTION

The idea that bed load transport rate of sediment grains in a fluid can be related to the energy expended on transporting the grains by the fluid flow in a stream was introduced by Bagnold (1956). He further extended this hypothesis to include the relationship between the interior flow and the suspended load transport rate (Bagnold 1963, 1966). As the grains are at different heights in the water column for the two modes of transport the forces acting on the grains are distinctly different. A mode dependent efficiency factor was introduced to account for this difference.

Bowen (1980) and Bailard (1981) independently developed a transport model for oceanic beaches based on the work of Bagnold. Bailard's model retained only the first two terms of the expansion of the velocity moments and assumes no autosuspension. The model predicts the total (i.e., bed and suspended load) longshore and cross-shore transport rate over an arbitrary bottom topography. Guza and Thornton (1985) analytically examined the relative importance of the velocity moments in Bailard's model using monochromatic and Gaussian velocity distributions, and compared these results with field measurements. They found modeling the nearshore velocity field as a linear, Gaussian, random process gave reasonable predictions for some moments and poor predictions of others.

Monochromatic waves gave poor predictions of the moments. They further found that mean flow and low frequency infragravity waves must be included to properly describe the velocity field for predicting sediment transport.

The principal aim of this paper is to evaluate the ability of Bailard's model to predict sediment transport from velocity data measured on a naturally barred beach. The data were acquired during the nearshore experiment Delilah and are composed of eight closely space velocity measurements extending from the shoreline to across the bar. The data are unique in that they were continuously recorded over a period of three weeks allowing examination of tidal effects. Since sediment transport was not measured directly, verification is by comparing predicted bathymetric changes to observed changes. A secondary goal is to determine the relative importance of forcing by mean currents, long waves and short waves under changing conditions over tidal cycles.

II. MODEL

Bailard's (1981) time averaged, immersed weight sediment transport rate, $\langle \vec{I}(t) \rangle$, is given by

$$\langle \vec{I}(t) \rangle = \rho C_f \frac{\epsilon_b}{\tan\phi}\left[\langle |\vec{u}(t)|^2 \vec{u}(t) \rangle - \frac{\tan\beta}{\tan\phi}\langle |\vec{u}(t)|^3 \rangle \hat{i}\right] + \rho C_f \frac{\epsilon_s}{W}\left[\langle |\vec{u}(t)|^3 \vec{u}(t) \rangle - \frac{\epsilon_s}{W}\tan\beta \langle |\vec{u}(t)|^5 \rangle \hat{i}\right] \quad (1)$$

where $|\vec{u}(t)| = [\tilde{u}^2 + \tilde{v}^2 + \overline{u}^2 + \overline{v}^2 + 2(\tilde{u}\overline{u} + \tilde{v}\overline{v})]^{\frac{1}{2}}$ is measured at the top of the bottom boundary layer, ρ is the water density, C_f is the bed drag coefficient, β is the beach slope, ϕ is the internal friction angle of the grains in the bed where $\tan\phi = 0.63$, and W is the fall velocity. The vector $\hat{i}$ is in the +x (offshore) direction. In equation (1) the terms in the first set of brackets represent the bed load contribution to total sediment transport and the terms in the second set of brackets represent the suspended load contribution. The suspended and bed load efficiency factors, ϵ_s and ϵ_b are the ratio of stream power to suspended and bed load work rates, respectfully.

Following Guza and Thornton (1985), the bi-directional velocity components are partitioned into oscillatory (tilde), and mean (overbar) flows

$$\vec{u}(t) = (\bar{u} + \tilde{u})\hat{i} + (\bar{v} + \tilde{v})\hat{j} \qquad (2)$$

Substitution of equation (2) into equation (1) gives equations for time averaged alongshore and cross-shore sediment transport rates. The equation of interest for our work is the cross-shore transport

$$\langle \vec{I}(x) \rangle = \rho C_f \frac{\epsilon_b}{\tan\phi} \left[\overset{1}{\langle \tilde{u}^3 \rangle} + \overset{2}{\langle \tilde{u}\tilde{v}^2 \rangle} + \overset{3}{\langle \tilde{u}^2 + \tilde{v}^2 \rangle \bar{u}} + 2 \overset{4}{\langle \tilde{u}^2 \rangle \bar{u}} + 2 \overset{5}{\langle \tilde{u}\tilde{v} \rangle \bar{v}} + \overset{6}{\bar{u}\bar{v}^2} + \overset{7}{\bar{u}^3} - \frac{\tan\beta}{\tan\phi} \overset{8}{\langle |\vec{u}(t)|^3 \rangle} \right]$$
$$+ \rho C_f \frac{\epsilon_s}{W} \left[\overset{9}{\langle |\vec{u}(t)|^3 \tilde{u} \rangle} + \overset{10}{\langle |\vec{u}(t)|^3 \bar{u} \rangle} - \frac{\epsilon_s}{W} \tan\beta \overset{11}{\langle |\vec{u}(t)|^5 \rangle} \right] \qquad (3)$$

The oscillatory terms $(\tilde{u}, \tilde{v})$ are further expanded into infragravity, $\tilde{u}_l$ (f<0.05 Hz), and incident, $\tilde{u}_s$ (f>0.05 Hz), wave components $\tilde{u}(t) = \tilde{u}_l(t) + \tilde{u}_s(t)$. Cross-shore transport was shown to be insensitive to the sign of longshore current. Determining the individual contribution by mean current, long and short wave is accomplished by allowing the contribution of interest and setting the other terms to zero (e.g., to find transport due only to the long wave component, u_l and v_l are as measured and u_s, v_s, $\bar{u}$, $\bar{v}$ = 0). This procedure eliminates cross terms that normally contribute to the transport.

In addition to partitioning the contributions to the sediment transport due to mean currents and oscillatory long

and short waves, the relative magnitudes of the eleven terms of equation (3) are also determined.

The volume sediment transport per unit width, q, (King and Seymour, 1986) is calculated from the immersed weight sediment transport per unit width, i

$$q = \frac{i}{(\rho_s - \rho)\, g} \tag{4}$$

where ρ_s = 2.65 gm/cm^3 is the density of quartz sand. To predict changes in bathymetry due to cross-shore transport it is assumed the bottom contours are straight and parallel and conditions are homogeneous alongshore such that $\frac{\partial q}{\partial y} = 0$. Conservation of mass is used to obtain an average change in depth between current meters due to cross-shore sediment flux

$$\mu \frac{\partial q}{\partial x}(x) = \frac{\partial h}{\partial t} \tag{5}$$

where μ = 0.7 is introduced to account for packing of the loose grains in the bed, and h is depth in meters.

III. DELILAH EXPERIMENT

Data were acquired as part of the DELILAH nearshore processes experiment at the Coastal Engineering Research Center's Field Research Facility (FRF) in Duck, NC during October 1990. The period investigated is from the morning of 8 October until the morning of 14 October. The environmental conditions are shown in Figure 1. This period was chosen because it contains both periods of relatively calm seas and storm conditions. Of note is the increased wind speed, significant wave height (HMO) and alongshore current during the storms commencing on 10 October and ending of the 13th. On the 10th, a frontal system from the south arrived resulting in waves up to 2m incident at relatively large angles (about 40 degrees from the south) driving strong northward longshore currents (up to 1.5 m/s). On the 13th, narrow band swell waves up to 2.5m arrived from hurricane Lili. Although these waves were larger, the incident wave angles were less and the resulting longshore currents were not as large.

The minigrid is defined as the area of bathymetry surveyed daily by the FRF's staff with the Coastal Research Amphibious Buggy (CRAB). The bathymetry before the large incident waves on 11 October shows significant variability alongshore and across-shore (Figure 2). The averaged (over 400m) bathymetry profiles during the experiment are shown in Figure 3. A tidal

plateau existed until the start of the storms when a well developed bar was formed. After the storms commencing on 11 October much of the alongshore variation has vanished and a linear longshore bar is present for the remainder of the experiment.

The velocity data used were obtained from a cross-shore array of bi-directional current meters located at about the center of the DELILAH minigrid (Figure 4). Also shown in Figure 3 are the location of current meters. The cross-shore distance in meters relative to the FRF coordinate system and depth relative to National Geodetic Vertical Datum (NGVD) are given in Table 1. Cross-shore distance and depths are in meters. Data from the most shoreward of current meters in the array, cm10, were not used as the sensor was frequently out of the water. At about 0700 on the 11th, cm60 was lost. From the 11th on, bathymetry predictions are averaged between cm50 and cm70 versus between cm50 to cm60 and from cm60 to cm70.

Velocity component data were numerically rotated to have axes parallel and perpendicular to depth contours. An average beach orientation was determined for each day based on the 2m contour averaged over about 400m alongshore. The rotation is such that the alongshore direction is defined in the direction of the 2m contour. The rotations for each day are given in Table 2. The wave induced horizontal velocities were depth corrected from sensor depth to the top of the bottom boundary layer to conform to the requirements of Bailard's model using

a transfer function based on linear wave theory, which is generally a good approximation

$$H(f) = \frac{1}{\cosh k(h + z_m)} \qquad (6)$$

where k is the wave number, h is the depth and z_m is the current measurement depth. Data from tide gage 511, located outside the surf zone near the 8m depth contour, were used to calculate the mean water level relative to NGVD to determine the 90 minute mean h in equation 6.

Typical energy density spectra are shown in Figure 5. It can be seen that there is a spectral gap at about 0.05 Hz which makes it a logical frequency to partition the data into long and short waves. This was done in order to determine the influence of different classes of waves on sediment transport.

Sediment ranged in size from about 0.12-0.2mm within the surf zone and consisted mostly of nearly spherical quartz. Cross-shore size distribution is shown in Table 3.

IV. APPLICATION OF MODEL

In the application of Bailard's model to field data, the efficiency factors ϵ_s and ϵ_b and the fall velocity, W, are specified based on mean grain size. The fall velocity for spherical quartz grains of mean size 0.2mm is 2 cm/sec (Dyer, 1986). A nominal $\epsilon_s \approx 0.015$ for a stream is used as determined by Bagnold (1966) and is used by others (e.g., Bowen 1980, Bailard 1981). Bagnold (1966) presents a functional relationship for ϵ_b with stream velocity and grain size. Using the mean grain size range of 0.12-0.2mm found at Duck (Table 3), and stream velocities with range of 1-2m/sec, $\epsilon_b \approx 0.135 \pm 0.004$, which indicates ϵ_b is not sensitive to the observed range of grain sizes or velocities.

A value of $C_f = 0.003$ was used which is the value obtained from longshore current modeling of the DELILAH data (Church and Thornton, 1993).

The values for $\tan\beta$ were calculated from the measured bottom slopes in the vicinity of each current meter.

The total immersed weight sediment transport partitioned into bed and suspended load components for current meters cm20-50 and cm80 are shown in Figures 6-10. Total cross-shore transport is simply the sum of bed and suspended load. Tidal variation in depth is superimposed on all graphs for comparison (tidal amplitudes are not to scale). Negative

transport indicates periods of onshore transport (accretion) and positive transport indicates offshore transport (erosion). Times of high energy (Figure 1) are easily discernable at each current meter location. Fluctuations in transport are roughly of the same period as the tide, although magnitude and phase vary with time and location. Transport due to suspended load is consistently greater than bed load, particularity during times of high waves (11 October, and 13 October).

Also shown is the transport due to mean, long wave and short wave components of the flow, also partitioned into bed and suspended load. As can be seen from equation (3), the components of the flow contribute non-linearly to the transport, and thus cannot merely be summed to equal the total.

The dominant forcing varies with location and conditions and will be discussed in order of increasing distance from the beach. In the area between the foreshore and trough (near cm20) there is very little accretion, with most of the erosion occurring during storm conditions. In this region, cross-shore transport is dominated by longshore and cross-shore mean flow. The short waves have a slightly greater influence than the long waves.

In the trough (Figure 7, cm30) the major events are accretionary. Short wave flow dominated the total transport in the trough during the second storm on 13 October.

On the shoreward slope of the bar (Figure 8, cm40) both accretion and erosion were evident with short wave component accretion usually dominating. Of note is that the long wave component produced mostly onshore transport.

On top of the bar (Figure 9, cm50) transport was almost exclusively offshore with mean and short wave flow nearly equal and both greater than long wave flow. In this area the periods of high transport rates were of greater duration than in any other area. A definite tidal period is seen here with mean and long wave flow contributions being predominantly during low tide and the short wave contribution being during transition from both low to high and high to low tide when the tidal currents can be expected to be at their maximum.

Further seaward at cm80 (Figure 10) transport is dominated by the short waves, and is confined to periods of very high waves.

Of particular interest are two cases in which the suspended and bed load transports are 180° out of phase. The first is at cm20 for the short wave flow component on the evening of the 13th. The second is at cm40 for the mean flow component at roughly the same time. The total suspended and bed load transport rates for these cases are in phase.

The contributions to the total transport by each of the eleven terms of equation (3) were evaluated by the model as well. As suspended load was calculated to be much greater than bed load, only one representative plot of the three

suspended load terms is shown (Figure 11). The dominance seems to vary between terms 9 and 11, depending on time and location. All three terms exhibited periods of positive and negative values and differing phase relationships between each other.

The daily predicted change in depth between current meter positions was determined using equations (4) and (5) (Figure 12) and compared with the observed bathymetric profiles. In the application of equation (5) to calculate the changes in the bathymetry, the sediment fluxes, calculated every 90 minutes are integrated (summed) between times of the bathymetry surveys (approximately every 24 hours) such that

$$\Delta h = \frac{\Delta t}{\Delta x} \sum_{t} [q(x_i, t) - q(x_{i+1}, t)] \qquad (7)$$

where Δt is the time between profile transects (nominally 24hrs) and $\Delta x = x_{i+1} - x_i$, the distance between current meters. An average profile was used to minimize the effect of longshore inhomogeneity. For each day, bathymetry profiles were averaged over 200m north and 200m south of the current meter array.

There is little discernable difference between predicted and observed depths from 8-9 October. A trough begins to form between cm20 and cm30 from 9-10 October. The model does not accurately account for this change. Between the 10th to 11th the trough continues to erode at an accelerated rate and the bar migrates to seaward. The model predicts a decrease in

depth between cm20 and cm30, opposite of the observed hollowing of the trough. The model does, however, indicate a deepening of the trough between cm30 and cm50. Between cm50 and cm60 the model correctly predicts the migration of the bar. During the low waves between the 11th and 12th there is little change in bathymetry, also reflected by the model. As the waves increase during the 12th to 13th the trough deepens and the bar migrates further seaward. The model again incorrectly shows a shallowing between cm20 and cm30, but correctly shows the trough deepening and seaward bar migration. From the 13th to 14th the model predicts much more transport than actually occurs. Interestingly, the transport is consistent with those days which did have significant change, (i.e., deepening of the trough and seaward migration of the bar).

V. DISCUSSION

Suspended load dominates bed load owing to the slow fall velocity (0.02m/s) of the fine grain sand (Table 1). This slow fall velocity means that the grains remain in suspension much longer with less turbulent energy required.

To a first order approximation, the model correctly predicts the deepening of the trough and offshore migration of the bar. However, in general, it under predicts changes in depth during low energy wave periods and over predicts during high energy episodes.

Between the foreshore and trough, transport is dominated by mean flow. The strong longshore current exerts a strong bottom stress while the weaker cross-shore flow (undertow) determines the direction of transport. The model consistently predicts a convergence in transport between cm20 and cm30, resulting in a decrease in depth. This is contrary to observed bathymetry changes. One possibility is that sediment is being transported out of the system by the longshore current. While only calculating the cross-shore component of sediment transport, one must assume that the longshore transport is constant and that any longshore variation in morphology can be averaged to a spatially constant mean profile. Averaging adjacent profiles may not be sufficient to account for divergences and convergence in the longshore

drift. As pointed out earlier, the bathymetry at the beginning of the experiment was significantly 3D (longshore and cross-shore variations) but evolved into a 2D configuration with a significant longshore bar after the storm on the 11th, Figure 2. This suggests that the assumption of longshore homogeneity was not always valid. Using only the cross-shore component of transport, particularly during times of 3D bathymetry, may not be sufficient to account for the observed changes in the bathymetry.

The calculated divergence of the sediment flux was not well resolved with the current meters separated by approximately 20m. Inspection of Figure 3 shows that cm20-50 positioning meant that the slope of the bottom changes sign at nearly each of these sensors. As term 11 of equation (3) is a function of this slope and one of the dominant terms, the calculated sediment flux for term 11 likewise changed sign at each current meter.

The model assumes that current velocities are taken near the top of the bottom boundary layer. The wave induced velocities were depth corrected using the linear wave theory transfer function (equation (6)). However, the mean currents were not depth corrected and substantial error could be introduced when considering the undertow.

Transition time from quiescence to high energy episodes as seen in Figure 1 is relatively short. During quiescent times the main influence on transport and bathymetry changes is by

the tide. Daily bathymetric transects are aliased over these times. Reducing the time between surveys to several times daily would provide bathymetry better suited to evaluate the model.

It was not possible to attribute the relative dominance between terms 9, 10, and 11 of equation (3) to any location or environmental condition as the terms varied greatly in time and space as well as relative phase. The only consistent feature was a definite tidal signature. That the tide is apparent in the model transport rates indicates that future measurements of sediment flux should be taken continuously over tidal cycles.

VI. CONCLUSIONS

Results indicate that suspended load was consistently greater than bed load during the DELILAH experiment, as much as an order of magnitude during episodes of large incident waves, due to the small grain size and resultant slow settling velocity.

The three velocity moments for suspended transport varied both spatially and temporally making evaluation of the dominant forcing components inconclusive.

The mean, long, and short wave contribution to the cross-shore sediment transport were all of the same order. The mean current forcing was dominated by the strong longshore current during the experiment with the cross-shore current at the bed determining the direction of the transport.

Variance of transport at all tide stages and during different wave conditions was much greater in the vicinity of the bar and trough. A tidal signature was evident throughout the cross-shore for each mode of flow suggesting that future experiments should acquire sediment flux data continuously over the tidal cycle, or that in predicting bathymetric changes the integration time step should resolve the tidal cycle.

Model predictions of bathymetric changes appear to under-predict measured bathymetry during low-energy periods and

over-predict during high-energy conditions. However, the model does correctly predict the first order movement of the bar.

Closer cross-shore placement of flow sensors in the vicinity of the trough and bar and several bathymetry measurements per day could result in more accurate representation of the transport processes and evaluation of the model.

APPENDIX A

TABLE 1. CURRENT METER cm10-90 CROSS-SHORE DISTANCE IN FRF COORDINATES AND DEPTH RELATIVE TO NGVD

Current Meter	Cross-shore distance (m) FRF	Depth (m) NGVD
cm10	125	0.07
cm20	145	-0.77
cm30	170	-.066
cm40	189	-.082
cm50	207	-.098
cm60	226	-1.01
cm70	245	-1.05
cm80	295	-1.66
cm90	370	-1.68

TABLE 2. ROTATION ANGLE FOR DEFINING ALONGSHORE DIRECTION

Date	Rotation angle
Oct 8	3.0
Oct 9	4.4
Oct 10	4.0
Oct 11	2.5
Oct 12	2.6
Oct 13	2.5
Oct 14	1.1

TABLE 3. SEDIMENT GRAIN SIZE ACROSS-SHORE

Cross-shore distance (m) FRF	Sediment mean diameter (mm)
138	.122
149	.182
192	.205
256	.143
328	.142
484	.158

APPENDIX B

Figures 1-12

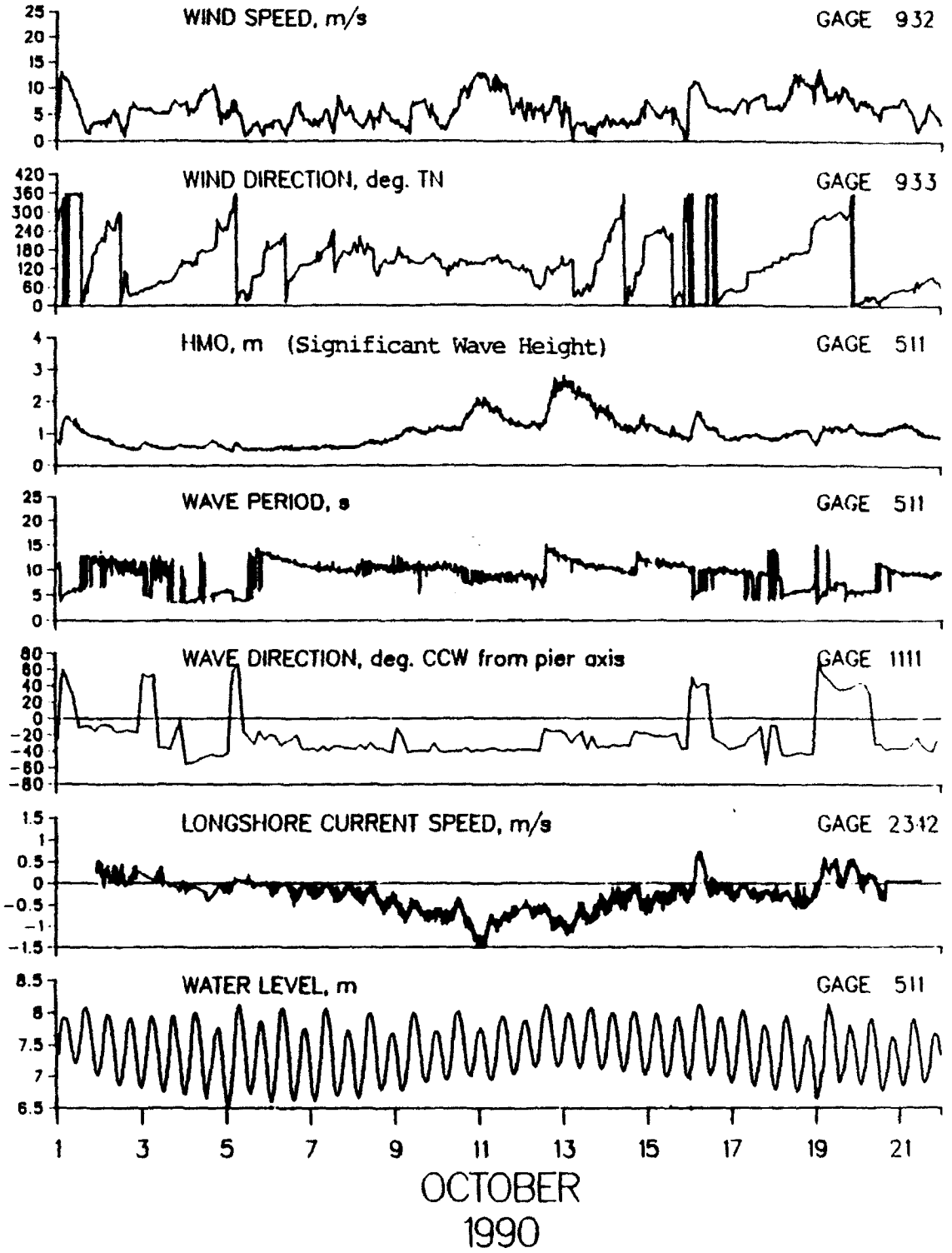

Figure 1. Environmental conditions during DELILAH. Period covered is morning of 8th to morning of 14th.

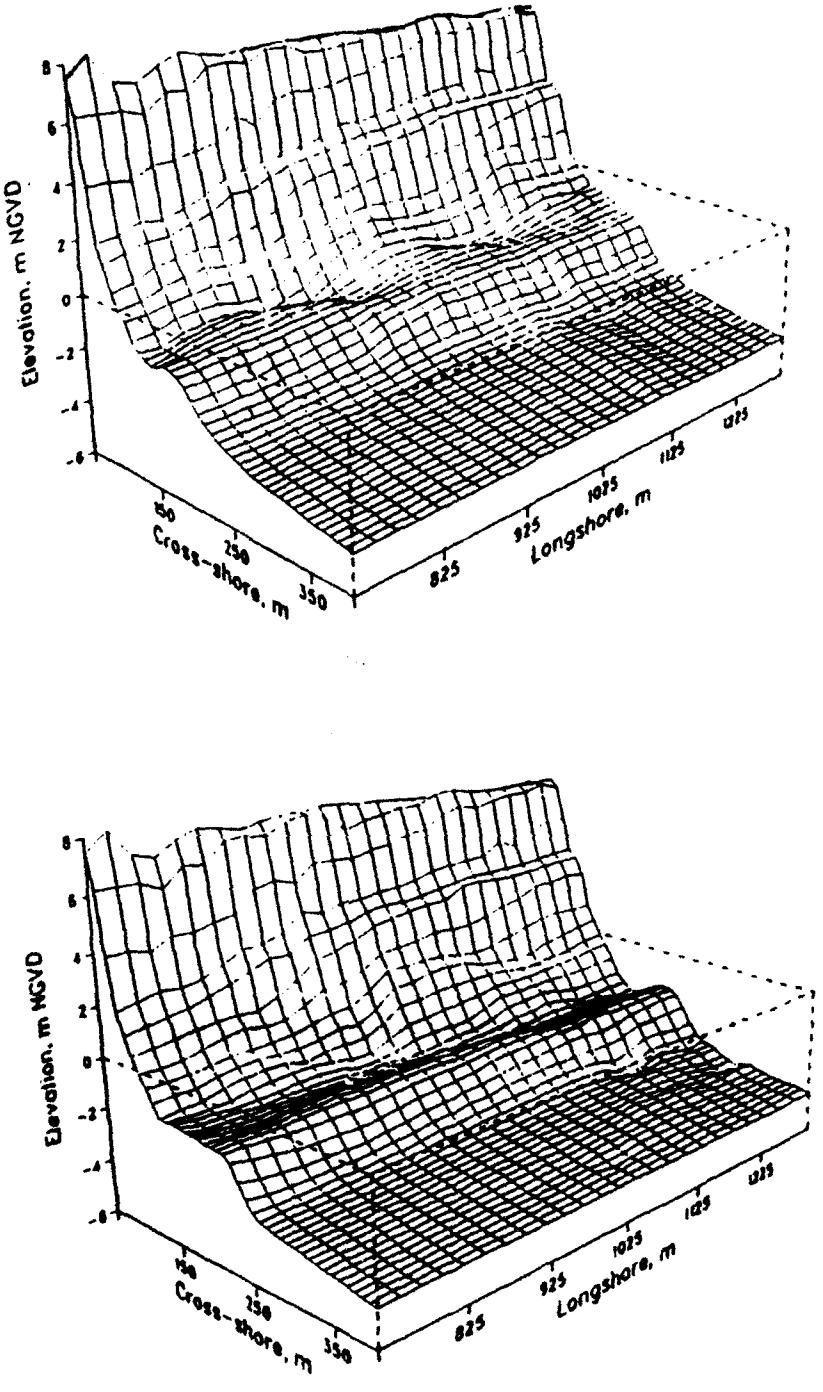

Figure 2. Minigrid 3D plot of bathymetry on 9 October (top) and 11 October (bottom) (from Birkemeir, Hathaway, Smith, Baron, Leffler, and many others, 1991).

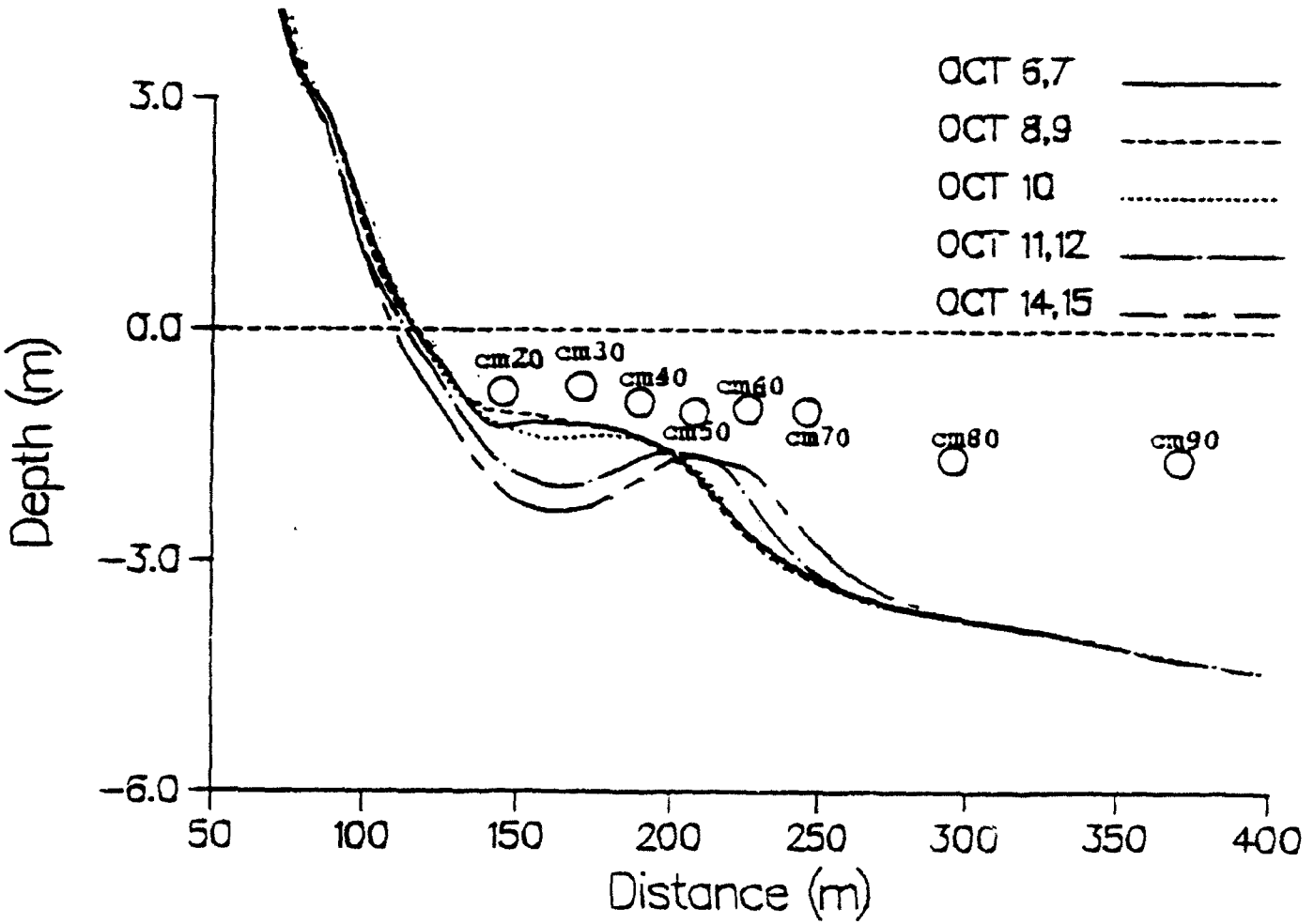

Figure 3. Location of current meters cm20 thru cm90 in the cross-shore and observed average bathymetry. Depths are relative to NGVD and cross-shore distances are in FRF coordinates.

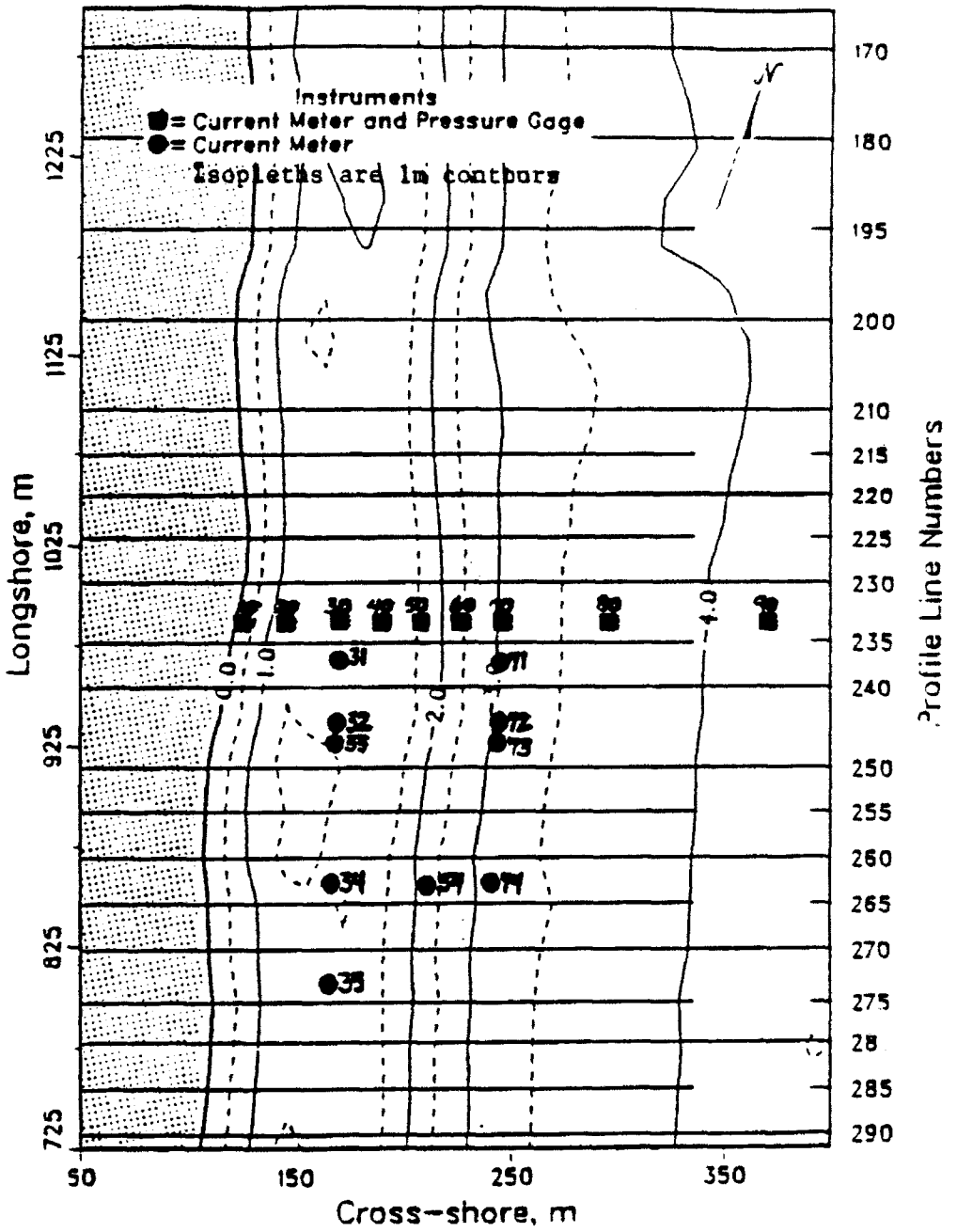

Figure 4. DELILAH minigrid. Longshore and cross-shore distances are in FRF coordinates (from Berkemeir, Hathaway, Smith, Baron, Leffler, and many others, 1991).

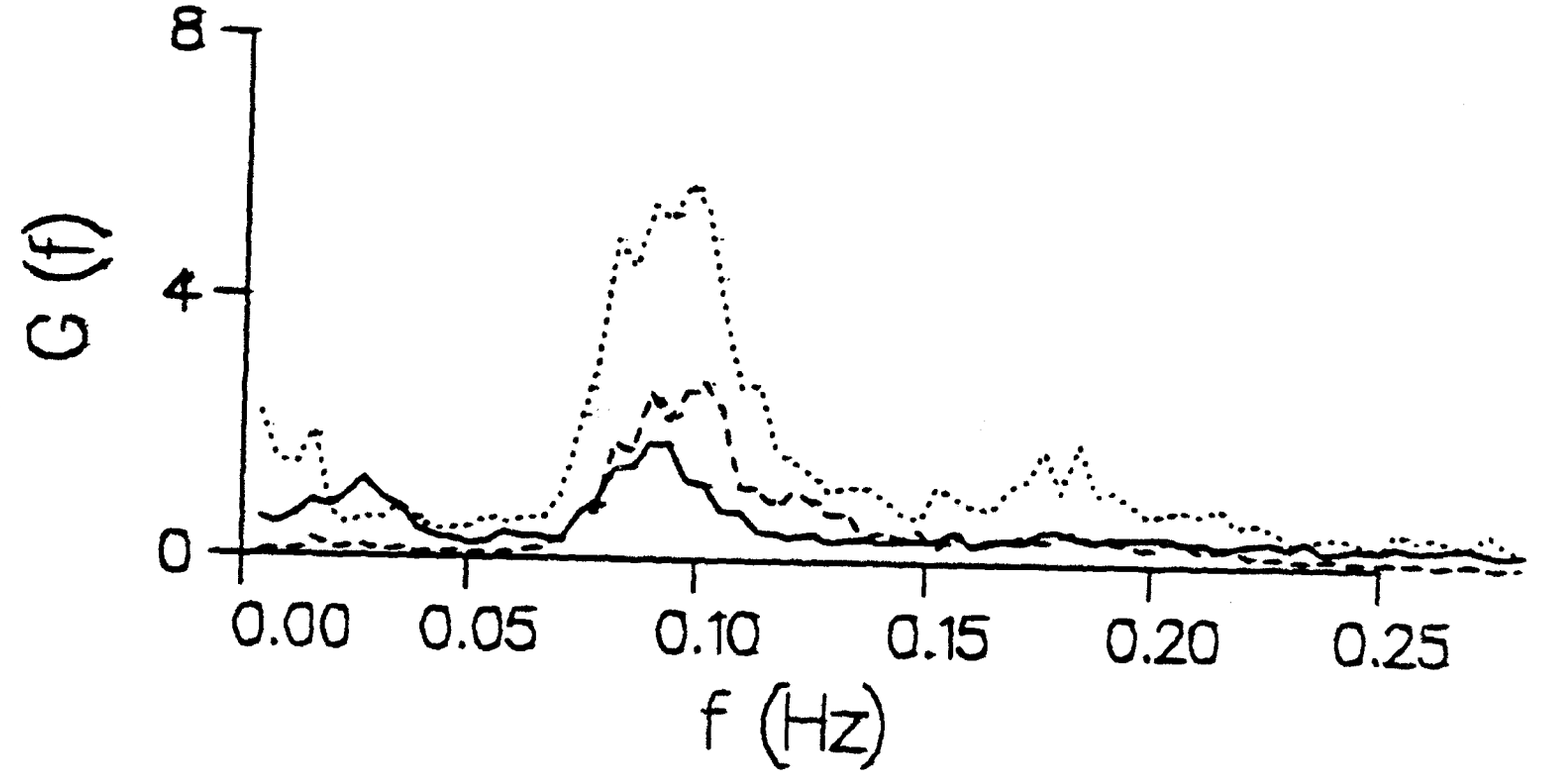

Figure 5. Spectral energy for the cross-shore component of the velocity on 9 October at three location across the surf zone. The solid line represents cm20, the dotted line cm50, and the dashed cm90 (from Scott and Thornton, 1991).

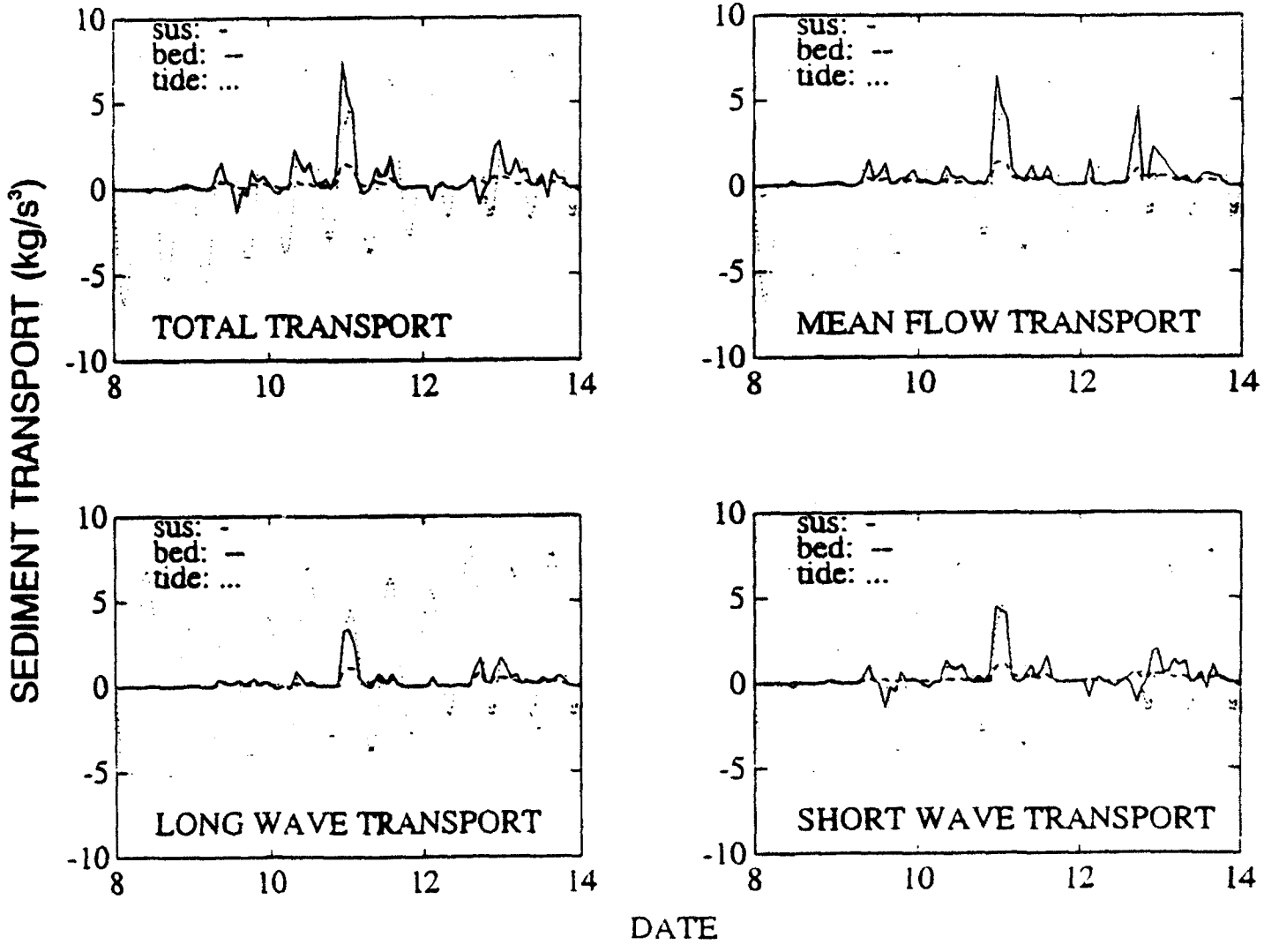

Figure 6. Immersed weight sediment transport per unit width at cm20. Upper left is the total, upper right due to mean currents, lower left due to long wave component of current, lower right due to short wave component of current. Each transport is partitioned into suspension and bed load. Tides are superimposed and amplitude is not to scale.

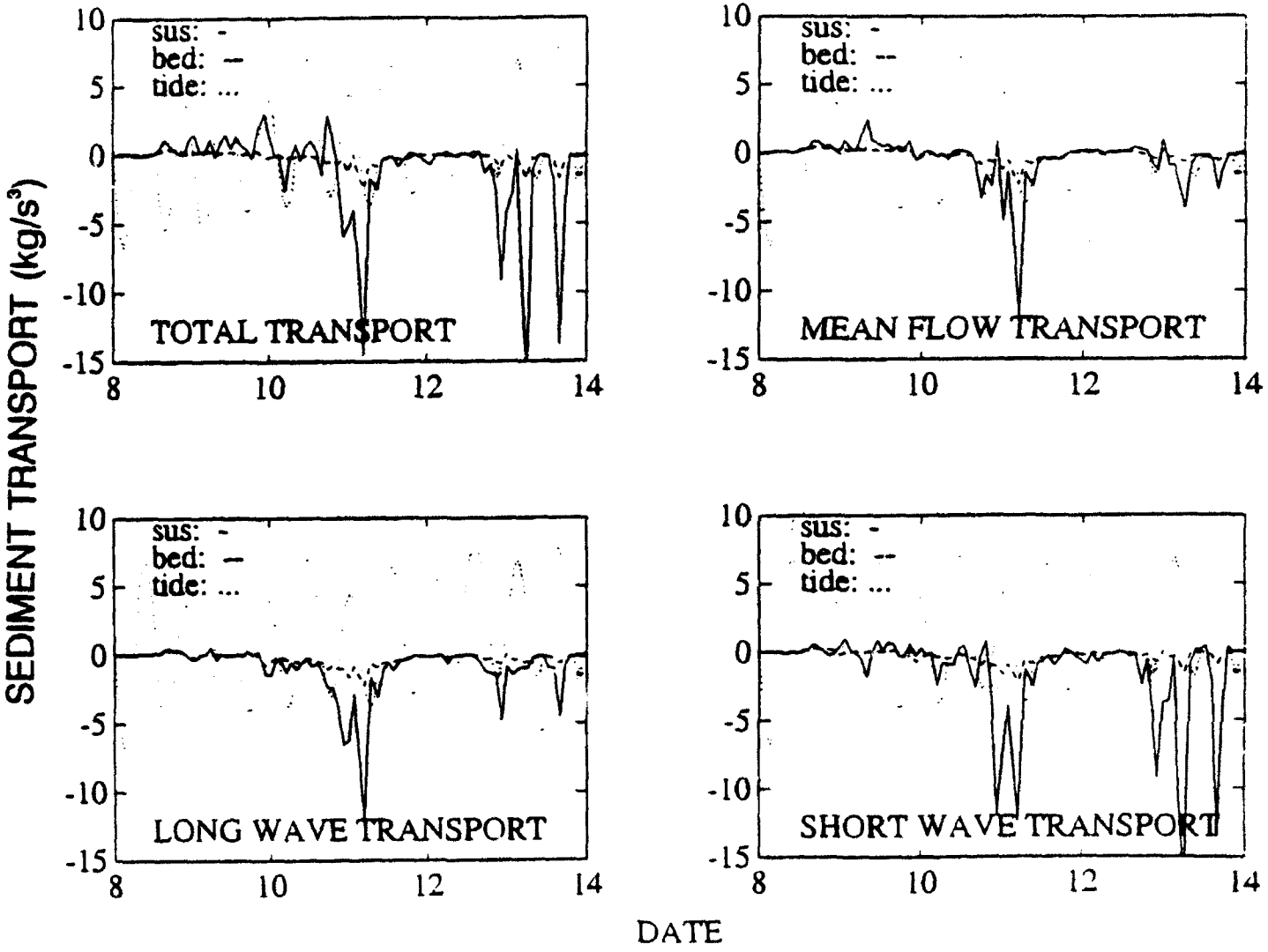

Figure 7. Immersed weight sediment transport per unit width at cm30. Upper left is the total, upper right due to mean currents, lower left due to long wave component of current, lower right due to short wave component of current. Each transport is partitioned into suspension and bed load. Tides are superimposed and amplitude is not to scale.

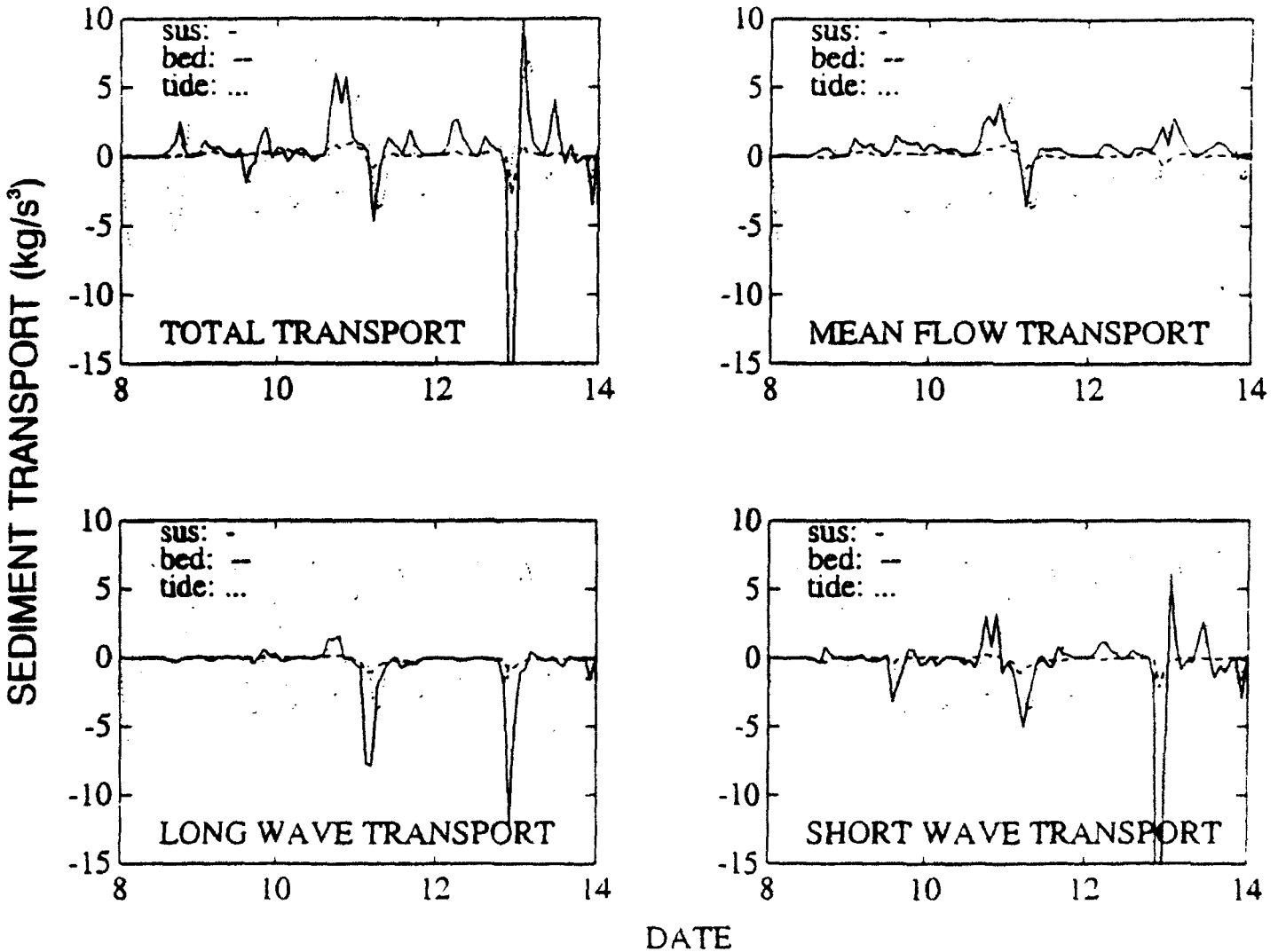

Figure 8. Immersed weight sediment transport per unit width at cm40. Upper left is the total, upper right due to mean currents, lower left due to long wave component of current, lower right due to short wave component of current. Each transport is partitioned into suspension and bed load. Tides are superimposed and amplitude is not to scale.

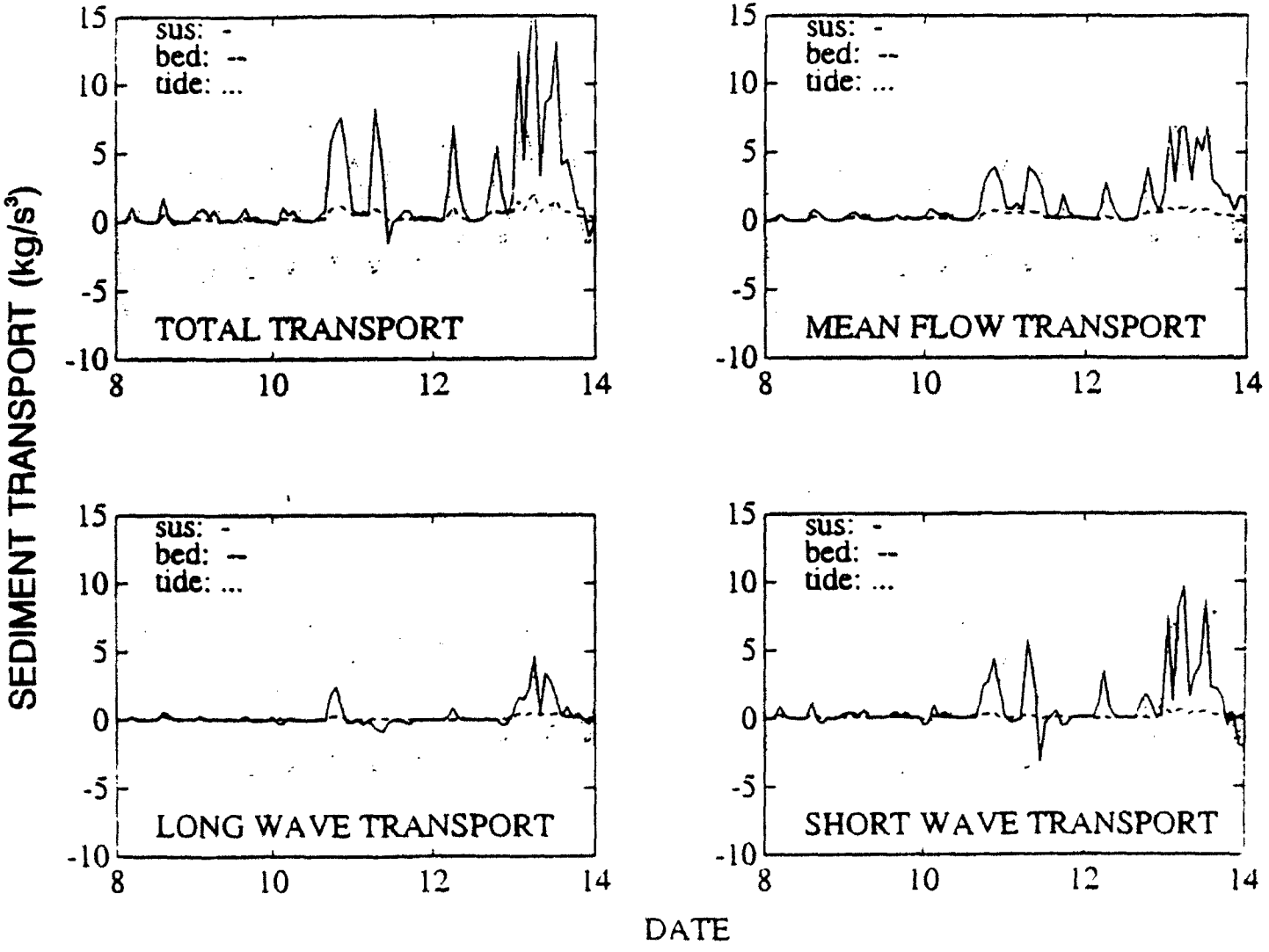

Figure 9. Immersed weight sediment transport per unit width at cm50. Upper left is the total, upper right due to mean currents, lower left due to long wave component of current, lower right due to short wave component of current. Each transport is partitioned into suspension and bed load. Tides are superimposed and amplitude is not to scale.

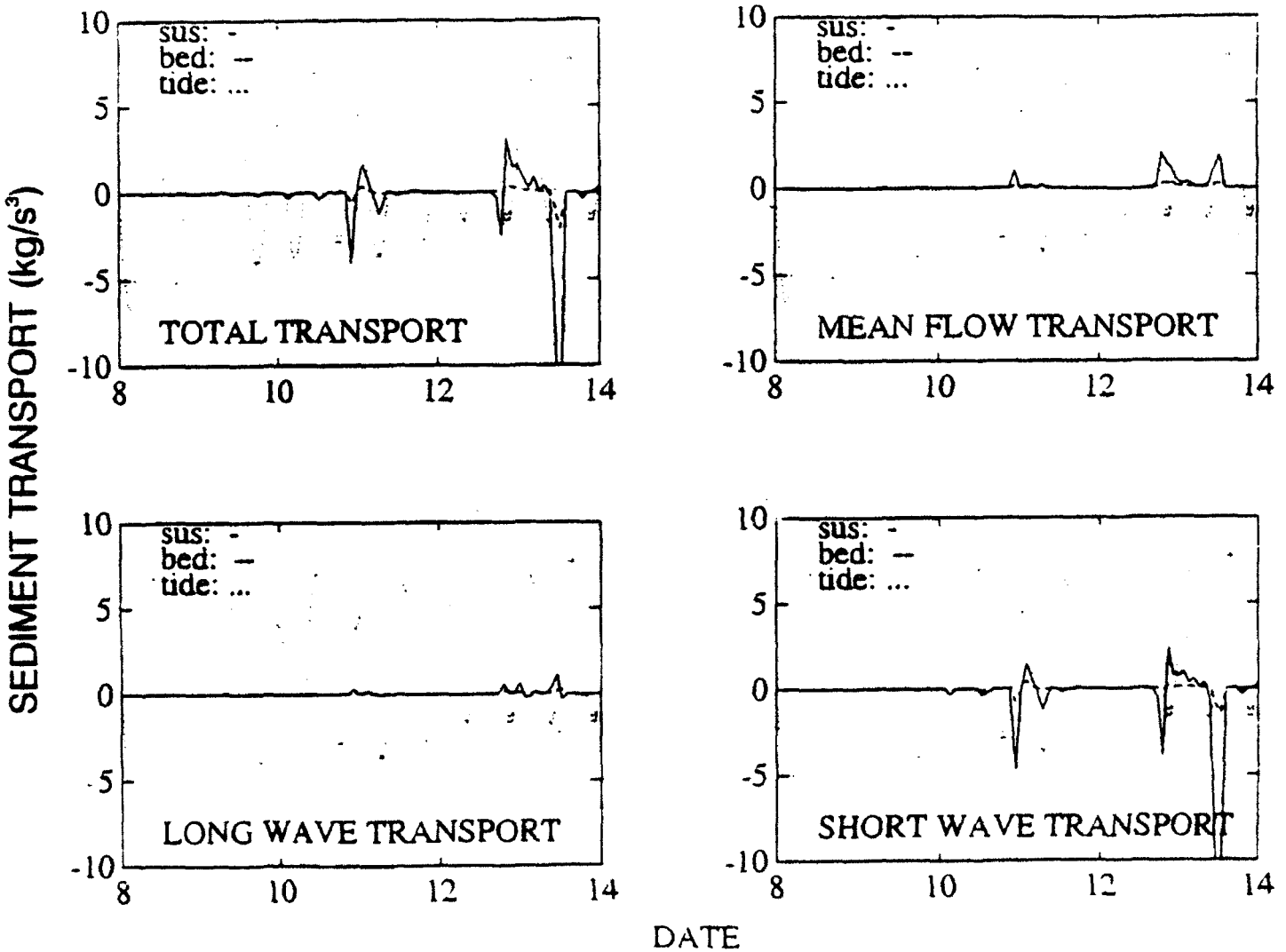

Figure 10. Immersed weight sediment transport per unit width at cm80. Upper left is the total, upper right due to mean currents, lower left due to long wave component of current, lower right due to short wave component of current. Each transport is partitioned into suspension and bed load. Tides are superimposed and amplitude is not to scale.

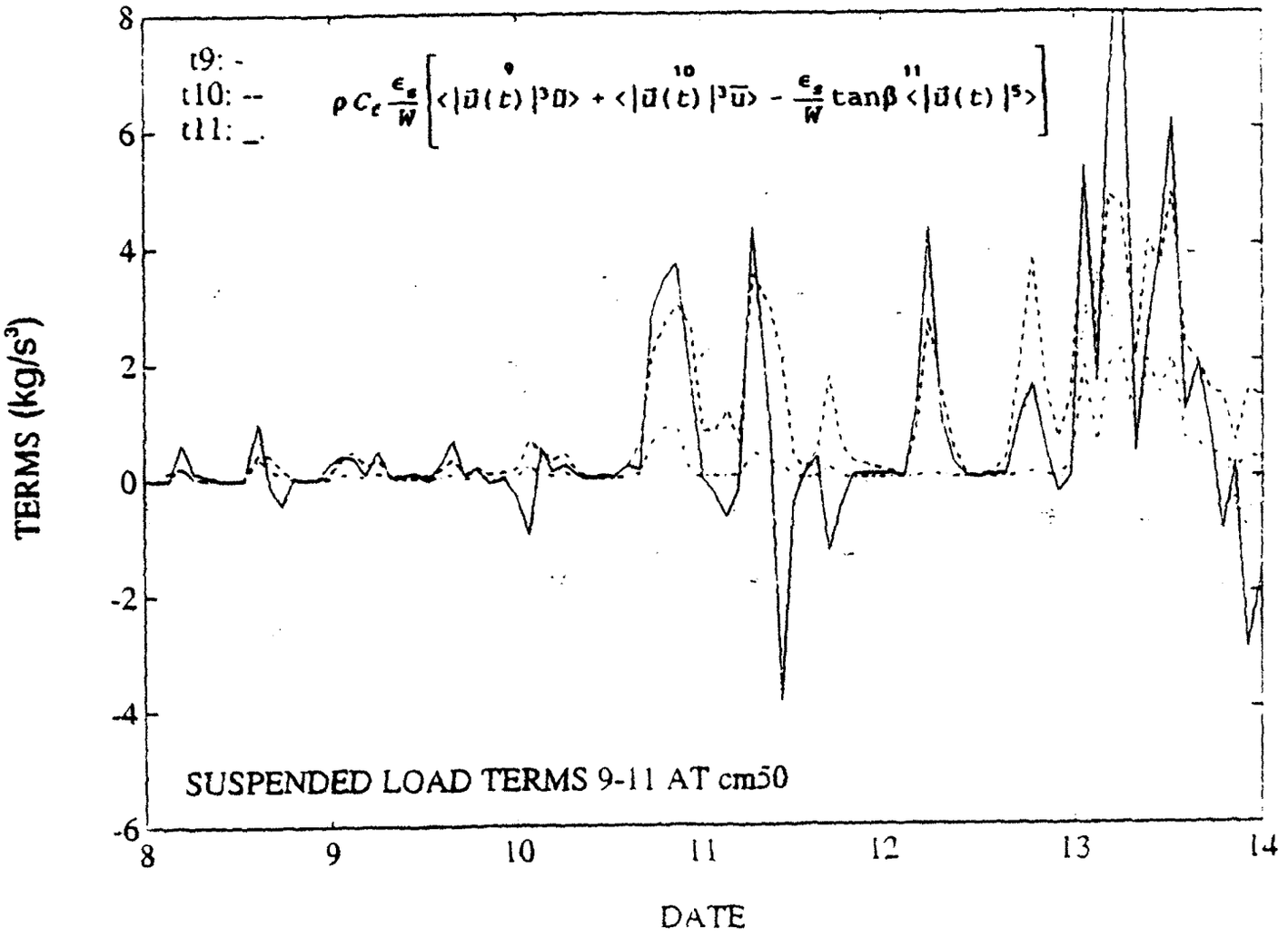

Figure 11. Model terms 9 thru 11 for cm50. Term 9 due to to ocillatory flow, term 10 due to mean flow and term 11 due to bottom slope. Tides are superimposed and amplitude is not to scale.

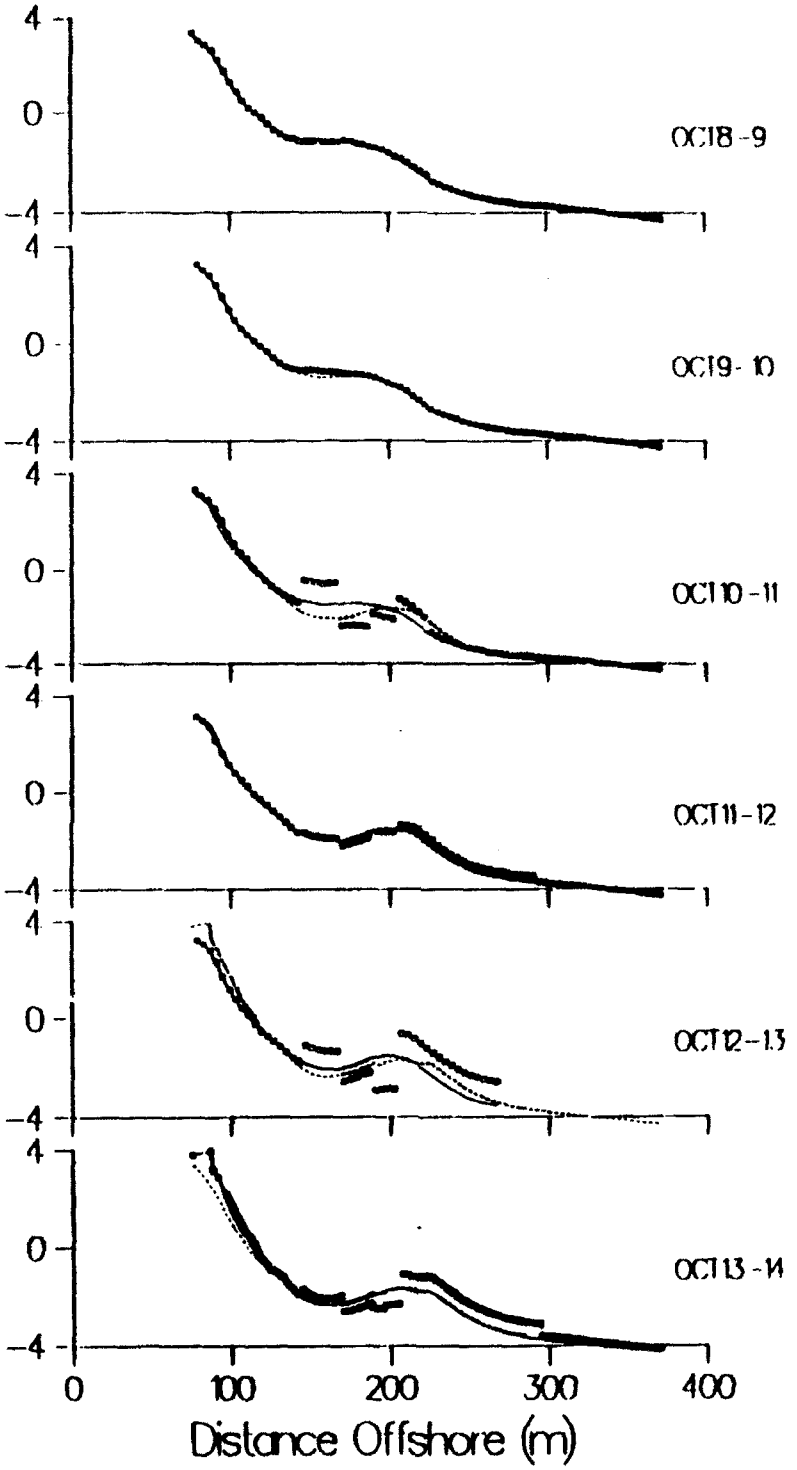

Figure 12. Predicted changes in bathymetry. Circles are predicted change over 24 hours to initial observed profile, solid line. Dotted line is observed profile 24 hours later. Given a perfect prediction, the circles would fall on top of the dotted line.

Page left blank on purpose

LIST OF REFERENCES

1. Bagnold, R. A., "Flow of Cohesionless grains in fluids." Royal Society [London] Philos. Trans., V. 249, pp. 235-297, 1956.

2. Bagnold, R. A., "Mechanics of Marine Sedimentation," in The Sea, Idea and Observations, V. 3, New York, N.Y., Interscience Publishers, pp. 507-528, 1963.

3. Geological Survey Professional Paper 422-I, An Approach to the Sediment Transport Problem From General Physics, R. A. Bagnold, 1966.

4. Naval Civil Engineering Laboratory Technical Note N-1626, An Energetics Total Load Sediment Transport Model For A Plane Sloping Beach, J. A. Bailard, April 1982.

5. Department of the Army, Waterways Experiment Station, Corps of Engineers, DELILAH Experiment: Investigator's Summary Report (draft), W. A. Birkemeier, et al, 1991.

6. Bowen, A. J., Simple models of nearshore sedimentation; beach profiles and longshore bars; in The Coastline of Canada, S.B. McCann, editor; Geological Survey of Canada, Paper 80-10, p. 1-11, 1980.

7. Church, J. C. and Thornton, E. B., "Effects of Breaking Wave Induced Turbulence Within a Longshore Current Model," (accepted in Journal of Coastal Engineering), 1993.

8. Dyer, K. R., Coastal and Estuarine Sediment Dynamics, 342 pp., John Wiley and Sons, 1986.

9. Guza, R. T., and E. B. Thornton, "Velocity moments in the nearshore," Journal of Waterway, Port, Coastal and Ocean Engineering, III(2), pp. 235-256, 1985.

10. King, D. B., Jr., and Seymour, R. J., Nearshore Sediment Transport, Chapter 16, "State of the art in oscillatory sediment transport models," pp. 371-385, Plenum Press, 418, 1989.

11. Scott, K. A., E. B. Thornton, and W. Birkmeier, Mean currents and sediment transport at DELILAH, Coastal Sediments, pp. 477-488, 1991.

INITIAL DISTRIBUTION LIST

		No. Copies
1.	Defense Technical Information Center Cameron Station Alexandria, VA 22304-6145	2
2.	Library, Code 52 Naval Postgraduate School Monterey, CA 93943-5002	2
3.	Chairman (Code OC/Co) Department of Oceanography Naval Postgraduate School Monterey, CA 93943-5000	1
4.	Chairman (Code MR/Hy) Department of Meteorology Naval Postgraduate School Monterey, CA 93943-5000	1
5.	Professor Edward B. Thornton (Code OC/Tm) Department of Oceanography Naval Postgraduate School Monterey, CA 93943-5000	2
6.	Commanding Officer Naval Western Oceanography Center Box 113 Pearl Harbor, HI 96860	1
7.	Office of Naval Research (Code 420) Naval Ocean Research and Development Activity 800 N. Quincy Street Arlington, VA 22217	1
8.	LT Randall T. Humiston Naval Western Oceanography Center P.O. Box 113 Pearl Harbor, HI 96860	2